This article was downloaded by: [Western Kentucky University]
On: 24 April 2013, At: 02:18
Publisher: Taylor & Francis
Informa Ltd Registered in England and Wales Registered Number: 1072954 Registered office: Mortimer House, 37-41 Mortimer Street, London W1T 3JH, UK

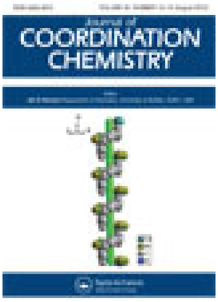

Journal of Coordination Chemistry
Publication details, including instructions for authors and subscription information:
http://www.tandfonline.com/loi/gcoo20

Two new lanthanide-radical complexes: synthesis, structure, and magnetic properties

Chao Wang [a], Ya-Li Wang [a], Yue Ma [a], Qing-Lun Wang [a], Li-Cun Li [a] & Dai-Zheng Liao [a b c]

[a] Department of Chemistry, Nankai University, Tianjin 300071, P.R. China

[b] Tianjin Key Lab on Metal and Molecule-based Material Chemistry, Nankai University, Tianjin 300071, P.R. China

[c] State Key Laboratory of Physical Chemistry of Solid Surface, Xiamen University, Xiamen 361005, P.R. China

Accepted author version posted online: 21 Jun 2012.Version of record first published: 06 Jul 2012.

To cite this article: Chao Wang, Ya-Li Wang, Yue Ma, Qing-Lun Wang, Li-Cun Li & Dai-Zheng Liao (2012): Two new lanthanide-radical complexes: synthesis, structure, and magnetic properties, Journal of Coordination Chemistry, 65:16, 2830-2838

To link to this article: http://dx.doi.org/10.1080/00958972.2012.705281

PLEASE SCROLL DOWN FOR ARTICLE

Full terms and conditions of use: http://www.tandfonline.com/page/terms-and-conditions

This article may be used for research, teaching, and private study purposes. Any substantial or systematic reproduction, redistribution, reselling, loan, sub-licensing, systematic supply, or distribution in any form to anyone is expressly forbidden.

The publisher does not give any warranty express or implied or make any representation that the contents will be complete or accurate or up to date. The accuracy of any instructions, formulae, and drug doses should be independently verified with primary sources. The publisher shall not be liable for any loss, actions, claims, proceedings, demand, or costs or damages whatsoever or howsoever caused arising directly or indirectly in connection with or arising out of the use of this material.

Journal of Coordination Chemistry
Vol. 65, No. 16, 20 August 2012, 2830–2838

Two new lanthanide–radical complexes: synthesis, structure, and magnetic properties

CHAO WANG†, YA-LI WANG†, YUE MA*†, QING-LUN WANG†, LI-CUN LI† and DAI-ZHENG LIAO†‡§

†Department of Chemistry, Nankai University, Tianjin 300071, P.R. China
‡Tianjin Key Lab on Metal and Molecule-based Material Chemistry, Nankai University, Tianjin 300071, P.R. China
§State Key Laboratory of Physical Chemistry of Solid Surface, Xiamen University, Xiamen 361005, P.R. China

(*Received 18 January 2012; in final form 7 May 2012*)

Two new lanthanide–radical complexes, $[Tb(hfac)_3(EtVNIT)_2]$ (**1**) and $[Dy(hfac)_3(EtVNIT)_2]$ (**2**) (EtVNIT = 2-(4′-ethoxy-3′-methoxyphenyl)-4,4,5,5-tetramethylimidazoline-1-oxyl-3-oxide, hfac = 1,1,1,5,5,5-hexafluoroacetylacetonate), were synthesized; both display radical–Ln(III)–radical (Ln=Tb (**1**), Dy (**2**)) tri-spin structures. Magnetic studies reveal that interactions between the lanthanide ions and radicals are ferromagnetic.

Keywords: Lanthanide ion; Nitronyl nitroxide radical; Crystal structure; Magnetic properties

1. Introduction

Since D. Gatteschi and co-workers discovered a family of rare-earth-based single-chain magnets [1–4] using nitronyl nitroxide radical and lanthanide ion, lanthanide–radical approach has been an effective method to obtain new single chain magnets [5–7] and single molecule magnets [8–14]. Terbium(III) and dysprosium(III) are generally selected as central ions [6–14] due to their large anisotropy. Constructing lanthanide–radical complexes using terbium(III) and dysprosium(III) remains relevant to explore the relationship between magnetic relaxation and coordination environments and the nature of the magnetic interactions between lanthanide ion and the spin carriers. Thus, we use 2-(4′-ethoxy-3′-methoxyphenyl)-4,4,5,5-tetramethylimidazoline-1-oxyl-3-oxide (EtVNIT) as radical ligand to coordinate with terbium(III) and dysprosium(III). EtVNIT chosen is very similar to the reported radical NITPhOEt [9], which constructs a mononuclear SMM with Tb(III). Our purpose is to examine the influence of different substituents of radical ligands (the adding of methoxy) on the magnetic properties of SMMs. Unfortunately, neither of the two complexes has magnetic ordering even at low temperature, but we evaluate the coupling between the central ion and the organic radicals in this article.

---

*Corresponding author. Email: maynk@nankai.edu.cn

Journal of Coordination Chemistry
ISSN 0095-8972 print/ISSN 1029-0389 online © 2012 Taylor & Francis
http://dx.doi.org/10.1080/00958972.2012.705281

Herein we reported the syntheses, crystal structures and magnetic properties of two new lanthanide–radical complexes, [Tb(hfac)$_3$(EtVNIT)$_2$] (**1**) and [Dy(hfac)$_3$(EtVNIT)$_2$] (**2**), showing radical–Ln(III)–radical (Ln=Tb (**1**), Dy (**2**)) tri-spin structures.

2. Experimental

2.1. *Materials and methods*

All commercial chemicals were used as received. The solvents were purified by standard methods. 2,3-Bis(hydroxylamino)-2,3-dimethylbutane was synthesized using the procedure described by Ullman [15]. Ln(hfac)$_3 \cdot 2H_2O$ (Ln=Tb, Dy, hfac = 1,1,1,5,5,5-hexafluoroacetylacetonate) was synthesized according to the literature [5]. Elemental analyses for C, H, and N were carried out on a Perkin-Elmer elemental analyzer (model 240). Variable temperature magnetic susceptibilities were measured on a SQUID MPMS XL-7 magnetometer from 2.0 K to 300 K at a magnetic field of 1000 Oe using polycrystalline samples. Alternating-current susceptibilities of **1** were measured under zero dc field at 1250 Hz from 2.0 to 20 K, while **2** was measured under 1000 Oe dc field at 1400 Hz from 2.0 to 20 K. Diamagnetic corrections were estimated from Pascal's constants for all constituent atoms.

2.2. *Synthesis of the radical EtVNIT*

EtVNIT is synthesized according to the literature [15], but slightly modified as follows: 2,3-bis(hydroxylamino)-2,3-dimethylbutane (2.96 g, 20.0 mmol) and 4-ethoxy-3-methoxybenzaldehyde (3.60 g, 20.0 mmol) were dissolved in 100 mL anhydrous methanol. This mixture was heated to reflux for 12 h, and then cooled to room temperature and stirred for 24 h. The slurry was filtered and washed with 5 mL cold methanol twice. Then the white powder was suspended in 150 mL CH_2Cl_2, cooled to 0°C, and then 150 mL water containing $NaIO_4$ (6.0 g, 28.1 mmol) was added to this suspension. The resulting mixture turned dark blue immediately and was stirred vigorously for 10 min at 0°C. Finally, the dark blue layer was collected and dried over anhydrous $MgSO_4$ overnight. After filtration to remove inorganic salts, the CH_2Cl_2 solution was evaporated to dryness and the residue was purified by column chromatography on silica gel (hexane : acetone = 3 : 1 as eluent). Yield: 4.59 g (74.7%). Elemental Anal. Calcd for $C_{16}H_{23}N_2O_4$ (307.36) (%): C, 62.52; H, 7.54; N, 9.11. Found (%): C, 62.12; H, 7.79; N, 9.30.

2.3. *Preparation of the lanthanide–radical complexes [Tb(hfac)$_3$(EtVNIT)$_2$] (1) and [Dy(hfac)$_3$(EtVNIT)$_2$] (2)*

[Tb(hfac)$_3$(EtVNIT)$_2$] (**1**): 80.8 mg (0.1 mmol) of Tb(hfac)$_3 \cdot 2H_2O$ was mixed with 25 mL *n*-heptane and this transparent solution was refluxed for 2 h. The resulting solution was cooled to 70°C, to which 30.7 mg (0.1 mmol) of EtVNIT and subsequently 10 mL of CH_2Cl_2 was added under stirring. After stirring for an additional hour, the final dark violet-blue solution was allowed to cool, filtered and kept at 4°C for one week. When the solution became colorless, dark blue block crystals were formed suitable for X-ray analysis. Yield: 27 mg (19% based on rare-earth element). Elemental Anal. Calcd for $C_{47}H_{49}F_{18}N_4O_{14}Tb$ (1394.81) (%): C, 40.47; H, 3.54; N, 4.02. Found (%): C, 40.31; H, 3.63; N, 4.09.

[Dy(hfac)$_3$(EtVNIT)$_2$] (**2**): Complex **2** was synthesized in similar manner, using Dy(hfac)$_3 \cdot 2H_2O$ instead of Tb(hfac)$_3 \cdot 2H_2O$. Yield: 29 mg (21%). Elemental Anal. Calcd for $C_{47}H_{49}F_{18}N_4O_{14}Dy$ (1398.38) (%): C, 40.37; H, 3.53; N, 4.01. Found (%): C, 40.48; H, 3.51; N, 3.94.

2.4. *X-ray structure determination*

Data were collected at 113(2) K on a Rigaku MM-007 single-crystal diffractometer equipped with a CCD area detector with graphite-monochromated Mo-Kα ($\lambda = 0.71070$ Å). A summary of crystallographic data is given in table 1. Empirical absorption corrections by semi-empirical from equivalents were carried out. The structure was solved with SHELX [16, 17] and refined by full-matrix least squares based on F^2 with anisotropic thermal parameters for the non-hydrogen atoms. Hydrogen atoms were located theoretically and refined isotropically. The selected bond lengths and angles are listed in tables 2 and 3 for **1** and **2**, respectively.

Table 1. Summary of crystal structure parameters for **1** and **2**.

	1	**2**
Empirical formula	$C_{47}H_{49}F_{18}N_4O_{14}Tb$	$C_{47}DyH_{49}F_{18}N_4O_{14}$
Formula weight	1394.84	1400.42
Crystal system	Monoclinic	Monoclinic
Space group	*C*2/*c*	*C*2/*c*
Unit cell dimensions (Å, °)		
a	21.7277(6)	21.712(5)
b	11.7635(3)	11.688(3)
c	22.8341(6)	22.748(5)
β	92.581(2)	92.273(3)
Volume (Å^3), *Z*	5830.3(3), 8	5768(2), 8
Calculated density (Mg m^{-3})	1.589	1.613
Absorption coefficient (mm^{-1})	1.333	1.417
F(000)	2792	2804
θ range (°)	2.4823–28.9877	1.792–27.879
Limiting indices	$-25 \le h \le 25$; $-14 \le k \le 9$; $-10 \le l \le 27$	$-25 \le h \le 24$; $-13 \le k \le 13$; $-26 \le l \le 7$
Reflections collected/unique	10,463/5185	19,407/5134
Completeness to θ	0.999	0.998
Max. and min. transmission	0.7213/0.6176	0.7457/0.6759
Goodness-of-fit on F^2	1.067	1.060
Final *R* indices [$I > 2\sigma(I)$]	$R_1 = 0.0306$ $wR_2 = 0.0351$	$R_1 = 0.0261$ $wR_2 = 0.0269$
R indices (all data)	$R_1 = 0.0768$ $wR_2 = 0.0781$	$R_1 = 0.0683$ $wR_2 = 0.0687$

Table 2. Selected bond lengths (Å) and angles (°) for **1**.

O(1)–Tb(1)	2.409(2)	O(2)–Tb(1)	2.3405(19)
O(3)–Tb(1)	2.3885(19)	O(4)–Tb(1)	2.344(2)
N(1)–O(4)	1.310(3)	N(2)–O(5)	1.270(4)
N(1)–O(4)–Tb(1)	133.67(17)	O(2)–Tb(1)–O(4)	97.44(7)
O(2)–Tb(1)–O(4)#1	95.64(7)	O(4)–Tb(1)–O(4)#1	143.45(10)
O(2)–Tb(1)–O(3)#1	147.50(7)	O(4)–Tb(1)–O(3)#1	72.70(7)
O(2)–Tb(1)–O(3)	75.05(7)	O(4)–Tb(1)–O(3)	77.99(7)
O(2)–Tb(1)–O(1)	72.83(7)	O(4)–Tb(1)–O(1)	144.23(7)
O(3)–Tb(1)–O(1)	129.05(7)	O(2)–Tb(1)–O(1)#1	72.98(7)
O(4)–Tb(1)–O(1)#1	72.32(7)	O(3)–Tb(1)–O(1)#1	132.42(7)
O(1)–Tb(1)–O(1)#1	71.92(10)		

Symmetry transformations used to generate equivalent atoms: #1: $-x, y, -z+1/2$.

Table 3. Selected bond lengths (Å) and angles (°) for **2**.

Dy(1)–O(1)	2.3263(17)	Dy(1)–O(2)	2.3972(17)
Dy(1)–O(3)	2.3751(17)	Dy(1)–O(6)	2.3301(16)
N(1)–O(6)	1.314(3)	N(2)–O(7)	1.270(3)
N(1)–O(6)–Dy(1)	133.66(14)	O(1)–Dy(1)–O(6)#1	96.69(6)
O(1)–Dy(1)–O(6)	96.27(6)	O(1)–Dy(1)–O(3)	74.65(6)
O(6)–Dy(1)–O(3)	72.29(6)	O(1)–Dy(1)–O(3)#1	147.27(6)
O(6)–Dy(1)–O(3)#1	78.36(6)	O(3)–Dy(1)–O(3)#1	72.97(8)
O(1)–Dy(1)–O(2)	73.30(6)	O(6)–Dy(1)–O(2)	72.51(6)
O(3)–Dy(1)–O(2)	128.59(6)	O(1)–Dy(1)–O(2)#1	72.91(6)
O(6)–Dy(1)–O(2)#1	144.17(6)	O(3)–Dy(1)–O(2)#1	132.84(6)
O(2)–Dy(1)–O(2)#1	71.66(8)	O(6)#1–Dy(1)–O(6)	143.32(8)

Symmetry transformations used to generate equivalent atoms: #1: $-x, y, -z+1/2$.

3. Results and discussion

3.1. *Synthesis and crystal structures of 1 and 2*

We followed syntheses of reported [Tb(hfac)$_3$(NITPhOEt)$_2$] [6], resulting in similar tri-spin molecules instead of the 1-D chain structures. We have repeated this experiment many times and measured the cell parameters, confirming that the tri-spin structures are more stable under these experimental conditions. Indeed, the molar ratio could explain the low yields of the reactions.

As shown in figure 1, the single-crystal X-ray analysis revealed that **1** is a tri-spin system consisting of one Tb(hfac)$_3$ and two EtVNIT molecules, the central Tb(III) is eight-coordinate by six oxygen atoms from three hfac units with Tb–O bond lengths of 2.341–2.409 Å and two oxygen atoms from two radical molecules with Tb–O(4) bond length of 2.344 Å, the coordination polyhedron can be described as a distorted dodecahedron with triangular faces in D_{2d} symmetry. The EtVNIT molecules are monodentate to Tb(III) through one N–O with N(1)–O(4) length of 1.310 Å, while the uncoordinated N(2)–O(5) bond length is 1.270 Å. As shown in figure 2, the shortest distance between uncoordinated oxygen atoms from radical units is 4.042 Å, while in **2**, the shortest distance is 4.059 Å. The X-ray analysis showed that these two complexes are isomorphous with replacement of the central ion causing little variation of crystal parameters, bond lengths, and bond angles.

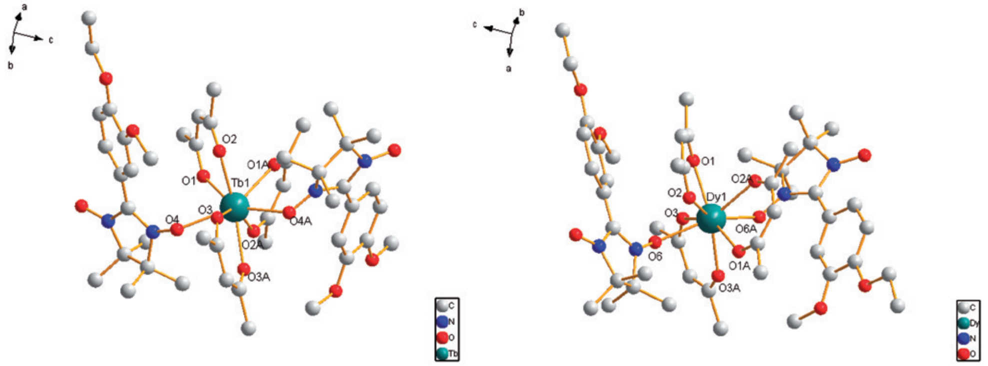

Figure 1. Molecular structure of **1** (left) and **2** (right) showing the coordination geometry of these tri-spin complexes. All hydrogen atoms and disordered fluorines are omitted for clarity.

3.2. *Magnetic properties*

The temperature dependence of the magnetic susceptibilities, $\chi_M T$ *versus* T plots for **1** and **2**, is shown in figure 3. For **1**, $\chi_M T$ at room temperature is $13.40\,\text{cm}^3\,\text{K}\,\text{mol}^{-1}$, which is a little higher than one uncoupled Tb(III) in the $^7F_6$ ground state ($\chi_M T = 11.81\,\text{cm}^3\,\text{K}\,\text{mol}^{-1}$) and two EtVNIT molecules ($S = 1/2$, $\chi_M T = 0.38\,\text{cm}^3\,\text{K}\,\text{mol}^{-1}$). The $\chi_M T$ value increases smoothly and reaches a maximum at 35 K with a value of $14.07\,\text{cm}^3\,\text{K}\,\text{mol}^{-1}$. Below 35 K, $\chi_M T$ begins to descend and sharply reaches a minimum of $12.14\,\text{cm}^3\,\text{K}\,\text{mol}^{-1}$ at 3.0 K. For **2**, at room temperature, $\chi_M T$ is $15.79\,\text{cm}^3\,\text{K}\,\text{mol}^{-1}$, somewhat higher than the expected value of uncoupled system of a Dy(III) ($^6H_{15/2}$, $g = 4/3$, $\chi_M T = 14.18\,\text{cm}^3\,\text{K}\,\text{mol}^{-1}$) and two EtVNIT molecules ($S = 1/2$, $\chi_M T = 0.375\,\text{cm}^3\,\text{K}\,\text{mol}^{-1}$). On cooling, $\chi_M T$ increases gradually and reaches a maximum of $19.51\,\text{cm}^3\,\text{K}\,\text{mol}^{-1}$ and then sharply reaches a minimum of $15.52\,\text{cm}^3\,\text{K}\,\text{mol}^{-1}$.

For these two complexes, there exist three kinds of magnetic interactions: (i) the coupling between lanthanide and the directly bonded radical, (ii) the interaction between two terminal radicals through the central lanthanide, and (iii) intermolecular interactions between the radicals due to short contacts highlighted in figure 2. However, because of the large anisotropy of terbium(III) and dysprosium(III), there are no available strict analytical expressions of magnetic susceptibility for these complexes. Therefore, to give a rough estimation of the magnetic interactions in these tri-spin molecules, we take **1** as an example and assume that the total magnetic susceptibilities χ can be calculated as a sum of an isolated Tb(III) and two uncoupled EtVNIT molecules (equation (1)), where all symbols have their usual meanings.

$$\chi = 2\chi_R + \chi_{Tb} = \frac{Ng_R^2\beta^2}{2kT} + \chi_{Tb}. \tag{1}$$

The Tb(III) has a $^7F_6$ ground state ($J = 6$) and may exhibit a splitting of the m_j energy levels ($\hat{H} = \Delta\hat{J}_Z^2$) in an axial crystal field. Thus, χ_{Tb} can be described by the expression (equation (2)) previously derived by Kahwa [18]. In this expression, Δ_1 is the

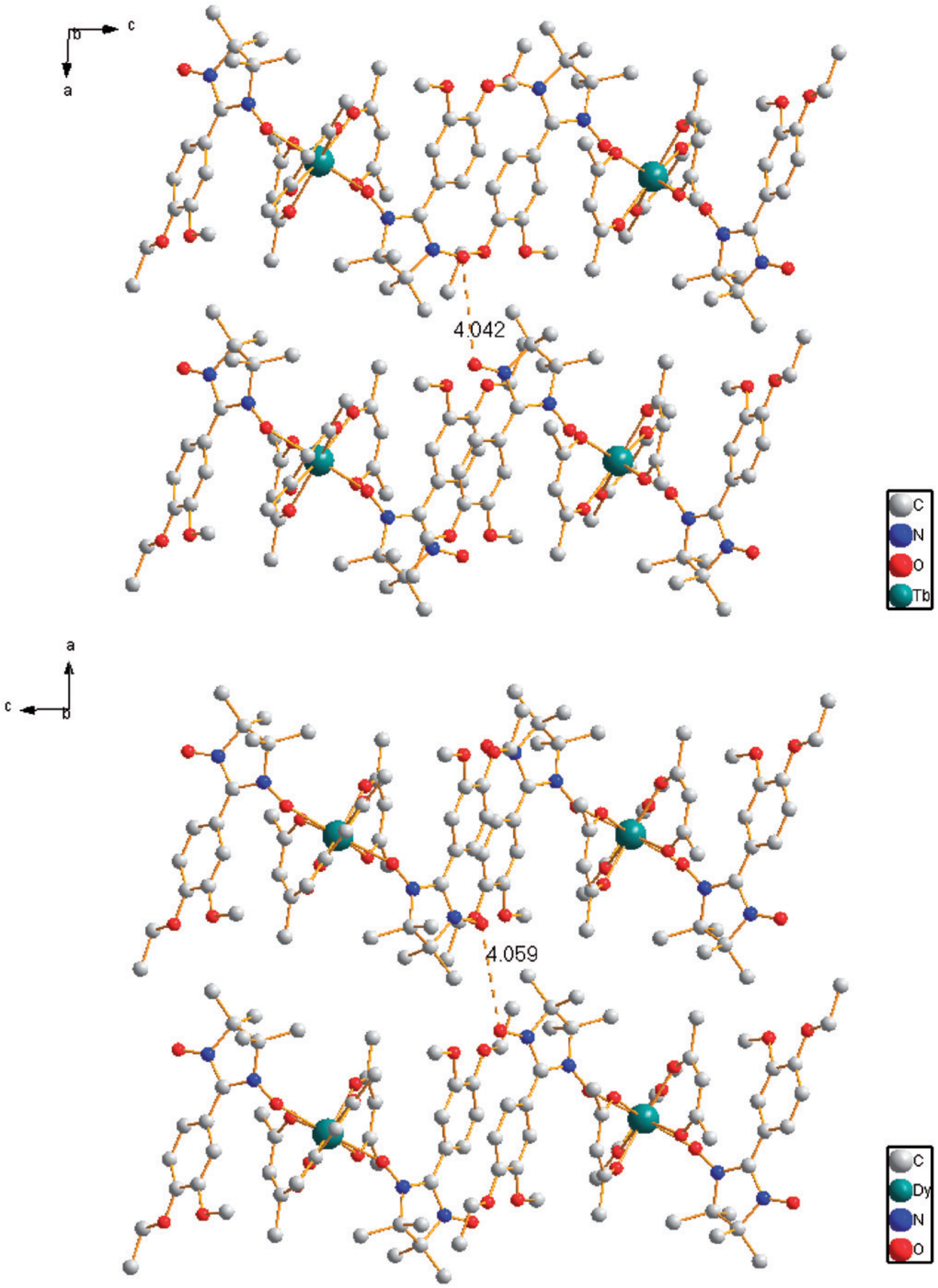

Figure 2. Packing arrangements of **1** (upper) and **2** (lower); these figures show that the shortest distances between uncoordinated oxygen atoms of the radical unit are 4.042 Å (in **1**) and 4.059 Å (in **2**). Hydrogen atoms and disordered fluorines are omitted for clarity.

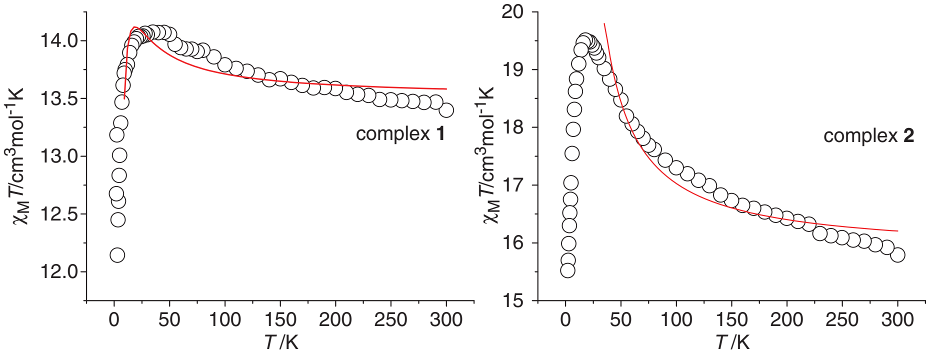

Figure 3. The temperature dependence of magnetic susceptibilities in the form of χ_M and $\chi_M T$ *vs.* T plots for **1** and **2**.

zero-field-splitting parameter:

$$\chi_{\mathrm{Tb}} = \frac{2Ng_1^2\beta^2}{kT}\left[\frac{\left\{\begin{array}{c}36\exp\left(\frac{-36\Delta_1}{kT}\right)+25\exp\left(\frac{-25\Delta_1}{kT}\right)+16\exp\left(\frac{-16\Delta_1}{kT}\right)+9\exp\left(\frac{-9\Delta_1}{kT}\right)\\ +4\exp\left(\frac{-4\Delta_1}{kT}\right)+\exp\left(\frac{-\Delta_1}{kT}\right)\end{array}\right\}}{\left\{\begin{array}{c}2\exp\left(\frac{-36\Delta_1}{kT}\right)+2\exp\left(\frac{-25\Delta_1}{kT}\right)+2\exp\left(\frac{-16\Delta_1}{kT}\right)+2\exp\left(\frac{-9\Delta_1}{kT}\right)\\ +2\exp\left(\frac{-4\Delta_1}{kT}\right)+2\exp\left(\frac{-\Delta_1}{kT}\right)+1\end{array}\right\}}\right]. \quad (2)$$

The molecular field approximation (zJ'_1) has been introduced to roughly evaluate the interactions between spin carriers and magnetic susceptibilities χ_1 can be calculated as

$$\chi_1 = \chi\left(1-\frac{2zJ'_1}{Ng_1^2\beta^2}\cdot\chi\right)^{-1}. \quad (3)$$

For **2**, the magnetic susceptibilities χ_2 can be calculated as for **1** [19–21]. The equations should be written as

$$\chi_2 = \chi\left(1-\frac{2zJ'_2}{Ng_2^2\beta^2}\cdot\chi\right)^{-1},$$

$$\chi = 2\chi_{\mathrm{R}} + \chi_{\mathrm{Dy}} = \frac{Ng_R^2\beta^2}{2kT} + \chi_{\mathrm{Dy}},$$

$$\chi_{\mathrm{Dy}} = \frac{Ng_2^2\beta^2}{4kT}\left[\frac{\left\{\begin{array}{c}225\exp\left(\frac{-225\Delta_2}{4kT}\right)+169\exp\left(\frac{-169\Delta_2}{4kT}\right)+121\exp\left(\frac{-121\Delta_2}{4kT}\right)+81\exp\left(\frac{-81\Delta_2}{4kT}\right)\\ +49\exp\left(\frac{-49\Delta_2}{4kT}\right)+25\exp\left(\frac{-25\Delta_2}{4kT}\right)+9\exp\left(\frac{-9\Delta_2}{4kT}\right)+\exp\left(\frac{-\Delta_2}{4kT}\right)\end{array}\right\}}{\left\{\begin{array}{c}\exp\left(\frac{-225\Delta_2}{4kT}\right)+\exp\left(\frac{-169\Delta_2}{4kT}\right)+\exp\left(\frac{-121\Delta_2}{4kT}\right)+\exp\left(\frac{-81\Delta_2}{4kT}\right)+\exp\left(\frac{-49\Delta_2}{4kT}\right)\\ +\exp\left(\frac{-25\Delta_2}{4kT}\right)+\exp\left(\frac{-9\Delta_2}{4kT}\right)+\exp\left(\frac{-\Delta_2}{4kT}\right)\end{array}\right\}}\right]. \quad (4)$$

The fittings were carried out from 10 to 300 K for **1** and 30 to 300 K for **2** due to the limit of the present model and complicated magnetic pathways. The parameters obtained in fitting are: $g_1 = 1.56$, $\Delta_1 = 0.32\,\mathrm{cm}^{-1}$, $zJ'_1 = 0.15\,\mathrm{cm}^{-1}$ (for **1**); $g_2 = 1.38$, $\Delta_2 = -0.052\,\mathrm{cm}^{-1}$, $zJ'_2 = 0.091\,\mathrm{cm}^{-1}$ (for **2**). The positive zJ' values in these two complexes suggest ferromagnetic coupling between Ln (Tb (**1**) or Dy(**2**)) ions and

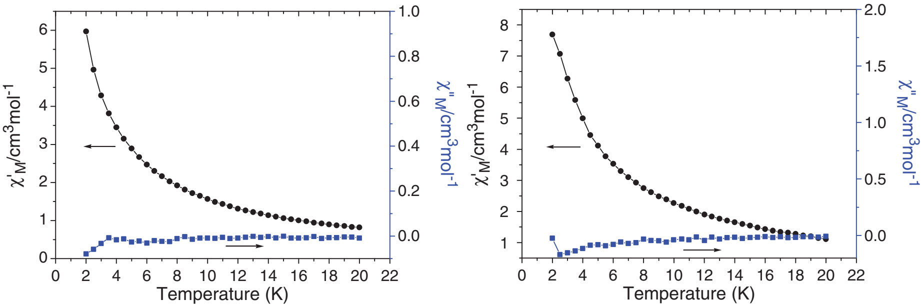

Figure 4. Temperature dependence of the in-phase (χ' round points) and out-of-phase (χ'' square points) components of the alternating-current susceptibility for **1** under zero dc field at 1250 Hz (left) and for **2** under 1000 Oe dc field at 1400 Hz (right).

nitronyl nitroxide radicals. The parameters of **1** are similar to a four-spin Tb-based lanthanide–radical complex [12], whose magnetic susceptibility was treated using the same simplified model. These two complexes, whose structures are very similar to reported SMMs [9, 22], were expected to be new SMMs. Therefore, alternating-current susceptibilities for these two complexes were carried out (as shown in figure 4), but unfortunately, we did not observe the signal of imaginary components (χ''_M) of these two complexes even at 2.0 K. Thus, we do not think **1** and **2** express magnetic ordering above 2.0 K.

In these reported radical–metal complexes, compared to transition metal ions [23, 24], lanthanide ions are usually employed to construct SMM due to their large unquenched angular momentum, but in this article, **1** does not express SMM behavior mainly due to the following reasons: first, the symmetry around lanthanide is D_{2d}, while the symmetry around lanthanide in [Tb(hfac)$_3$(NITPhOEt)$_2$] [9] and [Tb(hfac)$_3$(NITPhSMe)$_2$] [22] is D_{4d}, which could be the main factor to form SMM. Moreover, as mentioned above, in **1**, the shortest distance between the uncoordinated N–O moieties is 4.042 Å, which is shorter than that in [Tb(hfac)$_3$(NITPhOEt)$_2$] [9]. This shorter distance causes more significant intermolecular interactions, which might exclude the possibility of SMM. Compared to a reported complex [25], **2** is very similar to a tri-spin complex in bond lengths and bond angles, but $\chi_M T$ *versus* T curves express different tendencies. These behaviors might be caused by electron effects of sulfurs in [Dy(hfac)$_3$(NITPhSMe)$_2$] [25].

4. Conclusion

Two lanthanide–radical complexes with 2-(4′-ethoxy-3′-methoxyphenyl)-4,4,5,5-tetramethylimidazoline-1-oxyl-3-oxide as radical ligand were synthesized and characterized structurally and magnetically. Both complexes display radical–Ln(III)–radical tri-spin structures. Magnetic measurements reveal that the coupling between the central ion and the organic radicals are ferromagnetic.

Supplementary material

CCDC 848260 (**1**) and 848263 (**2**) contain the supplementary crystallographic data for this article. These data can be obtained free of charge from The Cambridge Crystallographic Data Centre *via* www.ccdc.cam.ac.uk/data_request/cif

Acknowledgments

This work was supported by the National Natural Science Foundation of China 21101096, 90922032, 21071085, 20971072, NSF of Tianjin 09JCYBJC05500, Research Fund for the Doctoral Program of Higher Education 20100031120013, and Fundamental Research Funds for the Central Universities.

References

[1] L. Bogani, C. Sangregorio, R. Sessoli, D. Gatteschi. *Angew. Chem. Int. Ed.*, **44**, 5817 (2005).
[2] K. Bernot, L. Bogani, A. Caneschi, D. Gatteschi, R. Sessoli. *J. Am. Chem. Soc.*, **128**, 7947 (2006).
[3] L. Sorace, C. Benelli, D. Gatteschi. *Chem. Soc. Rev.*, **40**, 3092 (2011).
[4] R. Sessoli, A.K. Powell. *Coord. Chem. Rev.*, **253**, 2328 (2009).
[5] K. Bernot, L. Bogani, R. Sessoli, D. Gatteschi. *Inorg. Chim. Acta*, **360**, 3807 (2007).
[6] R.N. Liu, L.C. Li, X.L. Wang, P.P. Yang, C. Wang, D.Z. Liao, J.P. Sutter. *Chem. Commun.*, **46**, 2566 (2010).
[7] R.N. Liu, Y. Ma, P.P. Yang, X.Y. Song, G.F. Xu, J.K. Tang, L.C. Li, D.Z. Liao, S.P. Yan. *Dalton Trans.*, **39**, 3321 (2010).
[8] G. Poneti, K. Bernot, L. Bogani, A. Caneschi, R. Sessoli, W. Wernsdorfer, D. Gatteschi. *Chem. Commun.*, 1807 (2007).
[9] N. Zhou, Y. Ma, C. Wang, G.F. Xu, J.K. Tang, J.X. Xu, S.P. Yan, P. Cheng, L.C. Li, D.Z. Liao. *Dalton Trans.*, 8489 (2009).
[10] H.X. Tian, R.N. Liu, X.L. Wang, P.P. Yang, Z.X. Li, L.C. Li, D.Z. Liao. *Eur. J. Inorg. Chem.*, 4498 (2009).
[11] X.L. Wang, L.C. Li, D.Z. Liao. *Inorg. Chem.*, **49**, 4735 (2010).
[12] J.X. Xu, Y. Ma, D.Z. Liao, G.F. Xu, J.K. Tang, C. Wang, N. Zhou, S.P. Yan, P. Cheng, L.C. Li. *Inorg. Chem.*, **48**, 8890 (2009).
[13] E. Coronado, C. Giménez-Saiz, A. Recuenco, A. Tarazón, F.M. Romero, A. Camón, F. Luis. *Inorg. Chem.*, **50**, 7370 (2011).
[14] K. Bernot, F. Pointillart, P. Rosa, M. Etienne, R. Sessoli, D. Gatteschi. *Chem. Commun.*, **46**, 6458 (2010).
[15] E.F. Ullman, J.H. Osiecki, D.G.B. Boocock, R. Darcy. *J. Am. Chem. Soc.*, **94**, 7049 (1972).
[16] G. Sheldrick. *SHELXS-97: Program for the Solution of Crystal Structures*, University of Göttingen, Germany (1997).
[17] G. Sheldrick. *SHELXL-97: Program for the Refinement of Crystal Structures*, University of Göttingen, Germany (1997).
[18] I.A. Kahwa, J. Selbin, C.J. O'Connor, J.W. Foise, G.L. McPherson. *Inorg. Chim. Acta*, **148**, 265 (1988).
[19] N. Xu, C. Wang, W. Shi, S.P. Yan, P. Cheng, D.Z. Liao. *Eur. J. Inorg. Chem.*, 2387 (2011).
[20] Y. Ouyang, W. Zhang, N. Xu, G.F. Xu, D.Z. Liao, K. Yoshimura, S.P. Yan, P. Cheng. *Inorg. Chem.*, **46**, 8454 (2007).
[21] N. Xu, W. Shi, D.Z. Liao, S.P. Yan, P. Cheng. *Inorg. Chem.*, **47**, 8748 (2008).
[22] X.L. Wang, X. Bao, P.P. Xu, L. Li. *Eur. J. Inorg. Chem.*, 3586 (2011).
[23] X.L. Wang. *J. Coord. Chem.*, **64**, 2215 (2011).
[24] X.H. Zhang, L. Guo, S.P. Wang, S.T. Yang, Y. Song. *J. Coord. Chem.*, **63**, 3198 (2010).
[25] X.L. Wang. *J. Coord. Chem.*, **64**, 4334 (2011).